The single-cell transcriptomic landscape of early human diabetic nephropathy

Parker C. Wilson[a], Haojia Wu[b], Yuhei Kirita[b], Kohei Uchimura[b], Nicolas Ledru[b], Helmut G. Rennke[c], Paul A. Welling[d], Sushrut S. Waikar[e], and Benjamin D. Humphreys[b,f,1]

[a]Department of Pathology and Immunology, Washington University in St. Louis, St. Louis, MO 63110; [b]Division of Nephrology, Department of Medicine, Washington University in St. Louis, St. Louis, MO 63110; [c]Department of Pathology, Brigham and Women's Hospital, Boston, MA 02115; [d]Department of Physiology, University of Maryland Medical School, Baltimore, MD 21201; [e]Division of Renal Medicine, Brigham and Women's Hospital, Boston, MA 02115; and [f]Department of Developmental Biology, Washington University in St. Louis, St. Louis, MO 63110

Edited by Martin R. Pollak, Beth Israel Deaconess Medical Center, Brookline, MA, and approved August 15, 2019 (received for review May 29, 2019)

Diabetic nephropathy is characterized by damage to both the glomerulus and tubulointerstitium, but relatively little is known about accompanying cell-specific changes in gene expression. We performed unbiased single-nucleus RNA sequencing (snRNA-seq) on cryopreserved human diabetic kidney samples to generate 23,980 single-nucleus transcriptomes from 3 control and 3 early diabetic nephropathy samples. All major cell types of the kidney were represented in the final dataset. Side-by-side comparison demonstrated cell-type–specific changes in gene expression that are important for ion transport, angiogenesis, and immune cell activation. In particular, we show that the diabetic thick ascending limb, late distal convoluted tubule, and principal cells all adopt a gene expression signature consistent with increased potassium secretion, including alterations in Na^+/K^+-ATPase, *WNK1*, mineralocorticoid receptor, and *NEDD4L* expression, as well as decreased paracellular calcium and magnesium reabsorption. We also identify strong angiogenic signatures in glomerular cell types, proximal convoluted tubule, distal convoluted tubule, and principal cells. Taken together, these results suggest that increased potassium secretion and angiogenic signaling represent early kidney responses in human diabetic nephropathy.

diabetic nephropathy | single cell | RNA-seq

Single-cell RNA sequencing (scRNA-seq) quantifies gene expression in individual cells (1), and unlike bulk RNA-seq, it can interrogate transcriptional states and signaling pathways in multiple cell types simultaneously. Advances in library preparation and isolation techniques, like single-nucleus RNA sequencing (snRNA-seq), have enabled the detection of rare cell types from cryopreserved samples (2). We hypothesized that snRNA-seq of kidney cortex in early diabetic nephropathy would reveal altered signaling pathways and gene expression patterns that would reflect the earliest adaptive changes to hyperglycemia.

Diabetic nephropathy is the leading cause of end-stage renal disease, but relatively little is known about early transcriptional changes that precede overt diabetic nephropathy. Laboratory measures like serum creatinine and urine protein are not sufficiently sensitive to detect the earliest manifestations of diabetic kidney disease, and efforts are underway to develop better biomarkers (3). Histologic signs of diabetic nephropathy include thickening of the glomerular basement membrane, mesangial expansion, and podocyte loss; however, the cell types and signaling pathways that contribute to disease progression are poorly understood (4). Previous efforts to characterize transcriptional changes in human diabetic glomeruli by bulk RNA-seq have identified important pathways, but are limited because they can only measure the integrated and averaged gene expression of multiple cell types (5–7).

Here, we describe an snRNA-seq analysis of early human diabetic nephropathy (8). We identified all major cell types in the kidney cortex and infiltrating immune cells in diabetic patients. The endothelium, mesangium, proximal convoluted tubule, and late distal convoluted tubule all had an angiogenic expression signature. We also observed changes in expression of the Na^+/K^+-ATPase and other transport-related genes in the thick ascending limb, distal convoluted tubule, and principal cells, indicative of enhanced urinary potassium secretion. These changes were accompanied by decreased expression of negative regulators of potassium secretion, *WNK1* and *NEDD4L*, and increased expression of the calcium-sensing receptor, *CASR*, and its downstream effector, *CLDN16*, suggestive of decreased paracellular calcium and magnesium reabsorption. Infiltrating immune cells were markedly increased in diabetic samples and expressed recently identified markers that predict diabetic nephropathy progression. These gene expression changes may be useful for identifying early biomarkers and signaling pathways in diabetic nephropathy.

Results

Kidney cortex was sampled from 3 nondiabetic controls and 3 diabetics following nephrectomy for renal mass. Diabetic patients had elevated A1c and evidence of mesangial sclerosis and glomerular basement membrane thickening (*SI Appendix*, Fig. S1). Patient age ranged from 52 to 74 y. Estimated glomerular filtration rate ranged from 56 to 85 mL/min/1.73 m^2 and was not different between groups. Two of three diabetic patients had proteinuria with an increased proportion of global glomerulosclerosis and interstitial fibrosis and tubular atrophy (IFTA) compared to controls (*SI Appendix*, Table S1). Differential gene expression and gene set enrichment analysis (GSEA) were performed between

Significance

Single-nucleus RNA sequencing revealed gene expression changes in early diabetic nephropathy that promote urinary potassium secretion and decreased calcium and magnesium reabsorption. Multiple cell types exhibited angiogenic signatures, which may represent early signs of aberrant angiogenesis. These alterations may help to identify biomarkers for disease progression or signaling pathways amenable to early intervention.

Author contributions: P.C.W. and B.D.H. designed research; P.C.W., H.W., Y.K., K.U., and S.S.W. performed research; P.C.W., H.W., N.L., H.G.R., P.A.W., S.S.W., and B.D.H. analyzed data; and P.C.W., P.A.W., S.S.W., and B.D.H. wrote the paper.

Conflict of interest statement: In separate work, B.D.H. consults for and receives grant support from Janssen to study mouse diabetic nephropathy. B.D.H. also consults for and holds equity in Chinook Therapeutics. Neither relationship is related to the contents of this manuscript.

This article is a PNAS Direct Submission.

Data deposition: The RNA-sequencing data reported in this paper are available on the Gene Expression Omnibus (accession no. GSE131882).

[1]To whom correspondence may be addressed. Email: humphreysbd@wustl.edu.

This article contains supporting information online at www.pnas.org/lookup/suppl/doi:10.1073/pnas.1908706116/-/DCSupplemental.

First published September 10, 2019.

the 2 diabetic patients with proteinuria and the patient without proteinuria (Datasets S2–S4). There was a trend toward increased serum potassium level in the diabetic group (4.2 ± 0.05 mEq/L) compared to controls (3.6 ± 0.32 mEq/L), but this was not statistically significant ($P = 0.12$).

snRNA-Seq Identifies All Major Cell Types in the Kidney Cortex. A total of 23,980 nuclei passed filters with an average of 2,541 genes and 6,894 unique molecular identifiers per nucleus (*SI Appendix*, Table S2). Eleven kidney cell types (Fig. 1 *A* and *B*) and four immune cell types (Fig. 1 *C* and *D*) were identified by unsupervised clustering and expression of lineage-specific markers following batch correction (*SI Appendix*, Fig. S2). Diabetics had an increased number of leukocytes consisting of T cells, B cells, monocytes, and plasma cells (Fig. 1 *C* and *D*). All data can be queried by users and visualized online at http://humphreyslab.com/SingleCell/.

Gene Expression Changes in the Diabetic Glomerulus. We identified differentially expressed genes in podocytes and mesangial and endothelial cells (Dataset S5). Approximately 10% of these transcripts have been previously reported in microarray studies of diabetic glomeruli from patients with more advanced disease (mean sCr = 2.83 ± 1.55 mg/dL) (6). There was no significant difference in podocyte number between diabetics (mean = 98 ± 15) and controls (122 ± 88, $P = 0.66$), although podocyte loss is an early feature of diabetic nephropathy (9). Our low sample number might explain the insignificant difference. Differential gene expression (Fig. 2*A*) and GSEA showed pathways important for regulation of endothelial cell proliferation and ion homeostasis (Datasets S6 and S7). *PLA2R1* and *THSD7A*, the targets of autoantibodies in primary membranous nephropathy, were increased in diabetic podocytes, in contrast to a prior report of later-stage diabetes where *PLA2R1* was down-regulated 6-fold (6). GSEA of the 2 diabetic patients with proteinuria compared to the diabetic patient without proteinuria showed enrichment of response to growth factors (Dataset S3), including up-regulation of *CTGF*, which has been previously implicated in diabetic nephropathy pathogenesis (10).

A total of 512 mesangial cells were identified, which likely represents an admixture of mesangial cells and vascular smooth muscle cells; both of which express *ITGA8* and *PDGFRB* (Human Protein Atlas). GSEA showed enrichment for GO biologic processes, including angiogenesis (Dataset S6), driven by increased expression of extracellular matrix components (*COL4A1*, *COL4A2*), and regulatory genes (*MYH9*, *NR4A1*, *SLIT3*, *ADAMTS12*). Decreased expression of *CFH* was observed in the cluster of cells defined by *CFH*, *CLDN1*, *VCAM1*, and *AKAP12*, which likely represent parietal epithelial cells.

A total of 1,179 endothelial cells were present, and GSEA identified enrichment for carbohydrate transport, leukocyte migration, and blood vessel endothelial cell migration. Differentially expressed genes (Fig. 2*C*) included extracellular matrix components (*COL4A1*), glucose transporters (*SLC2A3*, *SLC2A14*), and regulators of angiogenesis (*VEGFC*, *VCAM*, *NR4A1*, *MYH9*, *ITGB1*, *PRCP*, *TMEM204*, *HDAC9*, *MEF2C*) (11). The presence of an angiogenic signature in endothelial cells is consistent with prior reports in experimental diabetes, and aberrant glomerular angiogenesis is a feature of diabetic nephropathy associated with glomerular hypertrophy and increased expression of endothelial VEGF (11). *VEGFC* and *SEMA3D*, which belong to a class of genes called semaphorins that direct endothelial cell motility and vascular patterning, were both increased.

Altered Signaling Networks in the Diabetic Glomerulus. To explore alterations in intercellular signaling, differentially expressed ligand–receptor pairs were examined in glomerular cell types (Fig. 2*D*), which represent a subset of all interactions (Fig. 2 *E* and *F*). Diabetic mesangial cells had increased expression of *CCN1* and *SLIT3*. *CCN1* is a growth factor-inducible gene that regulates tissue repair via its interaction with extracellular proteins expressed by podocytes (*ITGAV*, *ITGB3*, *ITGB5*) and endothelial cells (*ITGB3*). *SLIT3* modulates cell migration by interacting with *ROBO2*, which is also expressed by podocytes and endothelial cells. Mesangial cells expressed *NAMPT*, which regulates insulin secretion in pancreatic β-cells, and diabetic podocytes showed decreased expression of *INSR*. Diabetic endothelial cells expressed increased *LTBP1*, which regulates targeting of latent TGF-beta complexes.

Infiltrating Immune Cells in Diabetic Nephropathy. A total of 347 leukocytes were identified and consisted of 49% T cells, 21% B cells, 23% monocytes, and 7% plasma cells (Fig. 1*C*). Diabetics had an approximate 7- to 8-fold increase in leukocytes compared to controls, which is consistent with previous reports (12). We did not detect a significant number of macrophages in diabetic samples, which is a potential limitation, because the role of macrophages in type 2 diabetic kidney disease is well-documented (12). Due to the small number of leukocytes present in controls, diabetic samples were compared to 2 publicly available peripheral blood mononuclear cell (PBMC) datasets (13, 14). Dataset integration identified NK cell, T cell, and monocyte subsets (*SI Appendix*, Fig. S3) and allowed us to measure changes in a panel of inflammatory markers (15). The kidney risk inflammatory signature (KRIS) is a recently described panel of 17 circulating plasma proteins that predict progression of diabetic nephropathy (15). We saw increased expression of *TNFRSF21* (LFC = 1.12, $P = 7.6e\text{-}58$) in the infiltrating diabetic CD14+ monocyte subset (Fig. 3*A*), which was one of the few KRIS markers that showed a correlation between enhanced urinary excretion and end-stage renal disease (15). *ILR1*

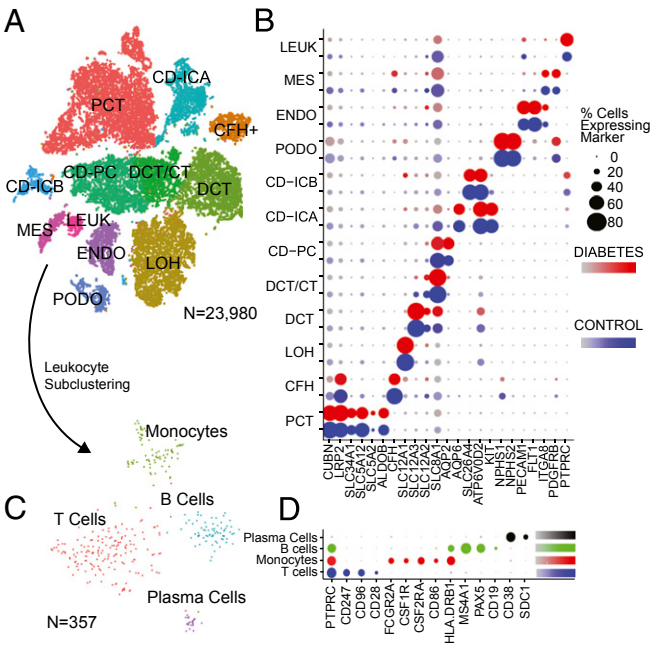

Fig. 1. Integrated snRNA-seq dataset of diabetic and control samples. (*A*) Diabetic and control samples were integrated into a single dataset and clustered using Seurat. PCT, proximal convoluted tubule; CFH, complement factor H; LOH, loop of Henle; DCT, distal convoluted tubule; CT, connecting tubule; CD, collecting duct; PC, principal cell; IC, intercalated cell; PODO, podocyte; ENDO, endothelium; MES, mesangial cell; LEUK, leukocyte. (*B*) Cell clusters were identified by kidney cell lineage-specific marker expression. (*C*) The leukocyte cluster (LEUK) was extracted from the integrated dataset and subclustered into leukocyte subsets. (*D*) Leukocyte subsets were identified by expression of lineage-specific markers.

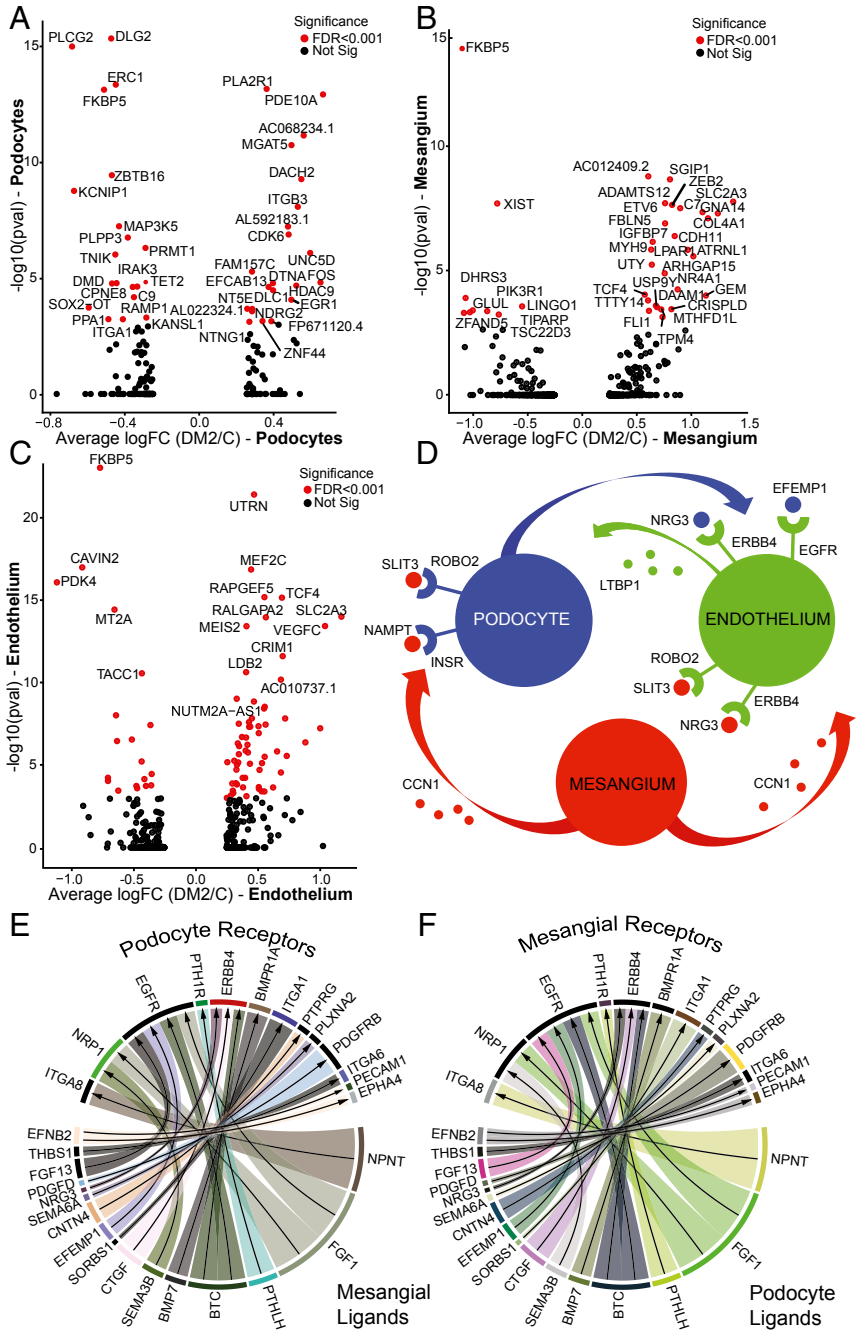

Fig. 2. Differential gene expression and intercellular signaling in the diabetic glomerulus. Diabetic and control samples were integrated into a single dataset, and gene expression was compared within cell types using Seurat. Differentially expressed genes are displayed for (*A*) podocytes, (*B*) mesangial cells, and (*C*) endothelial cells. Ligand–receptor interactions were inferred using a publicly available database (Ramilowski et al., ref. 44) and include (*D*) differentially expressed ligand–receptor intercellular signaling pathways and (*E* and *F*) all possible ligand–receptor signaling pathways in the podocyte and mesangium. FDR, false discovery rate.

was increased in CD16+ monocytes and antigen presenting cells, and *IL18R1* was increased in CD4+ and CD8+ T cells. These data suggest that infiltrating immune cells contribute to the production of KRIS markers.

Gene Expression Changes in the Diabetic Proximal Convoluted Tubule and Thick Ascending Limb. The proximal convoluted tubule (PCT) had 6,518 cells and was enriched for regulation of IL-8 production and angiogenesis. The diabetic PCT had increased expression of the albumin transporter, *LRP2*, and regulators of angiogenesis: *NRP1*, *VCAM1*, and *HIF1A* (16). There was a shift in metabolism characterized by up-regulation of *PCK1* and down-regulation of *INSR*. Phosphoenolpyruvate carboxykinase 1 (PCK1) is a control point for regulation of gluconeogenesis (17) and ammoniagenesis (18).

The thick ascending limb (TAL) had 3,788 cells and was enriched for regulation of sodium ion transmembrane transporter activity, regulation of potassium ion, and cell junction assembly (Dataset S8). Na^+/K^+-ATPase (NKA) subunits encoded by *ATP1A1*, *ATP1B1*, and *FXYD2* (19) were decreased. *WNK1* and its downstream effector, *STK39*, were also decreased, which regulate Na^+-K+-2Cl− cotransporter (NKCC2), albeit modestly (20).

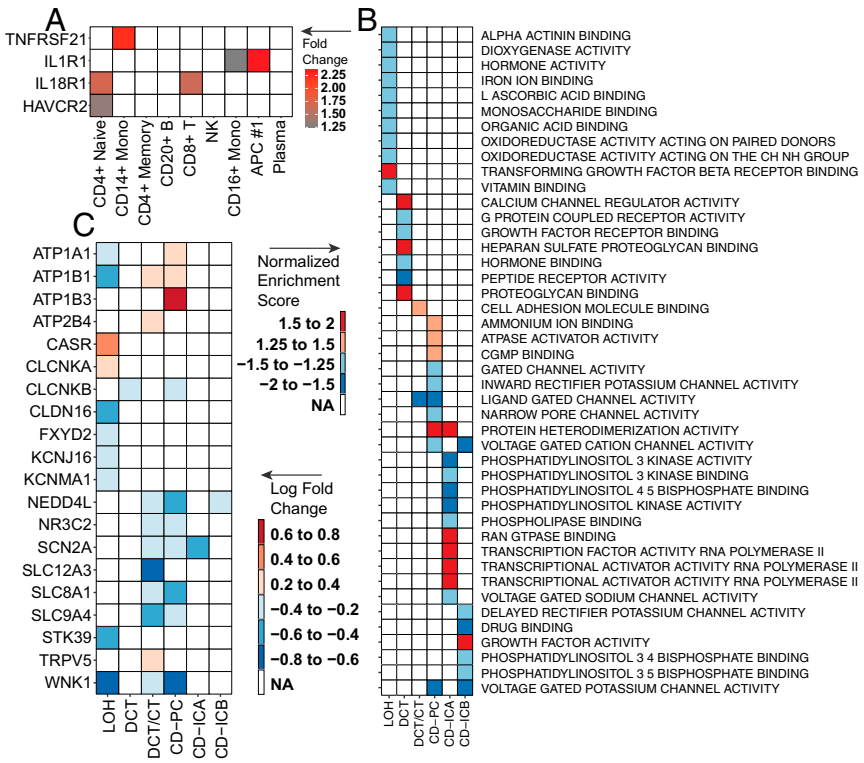

Fig. 3. Differential expression of predictive biomarkers and ion transport pathways. (*A*) Leukocyte subsets extracted from the integrated dataset were interrogated for differential expression of a panel of inflammatory markers (KRIS). (*B*) Cells from the loop of Henle (LOH) to the collecting duct underwent gene set enrichment analysis using the R package fgsea and were mapped to gene ontology terms. (*C*) Differentially expressed genes involved in ion transport in the distal nephron were identified using Seurat.

Nevertheless, because sodium and potassium transport in the TAL are driven by the in-series operation of NKCC2 and the NKA, these changes are expected to reduce Na^+ and K^+ reabsorption. Inhibition of transport in the TAL is expected to be compounded by the reduction in the basolateral potassium channel, *KCNJ16*, and an increase in the calcium-sensing receptor, *CASR*, which inhibits Na^+-K^+ reabsorption and drives calcium excretion by decreasing NKCC2, the ROMK channel (21), and CLDN16, which forms tight junctions by oligomerizing with CLDN19 (22). *CLDN16* was decreased, which leads to increased sodium delivery to the collecting duct, increased fractional excretion of potassium, and impaired calcium and magnesium reabsorption (23, 24).

Diabetes Induces Gene Expression Changes That Promote Potassium Secretion in the Late Distal Convoluted Tubule and Principal Cells. The late distal convoluted tubule had 1,652 cells, enriched for regulation of ion transport, calcium-mediated signaling, and response to steroid hormones. Increased expression of the apical calcium-selective channel, *TRPV5*, and the basolateral plasma membrane calcium ATPase (PMCA), *ATP2B4*, likely result as a consequence of reduced calcium transport in the TAL (Fig. 3*C*) (25) There was also decreased *NEDD4L* and increased *SGK1*, which promote surface expression of ENaC.

A total of 2,909 principal cells were enriched for regulation of distal tubule development, potassium ion transport, sodium ion transport, and response to hormone (Dataset S8). Diabetic principal cells had increased expression of *ATP1A1*, *ATP1B1*, *ATP1B3*, and the modulator *FXYD4*, which increases NKA affinity for Na^+ and K^+ (Fig. 3*C*). Immunofluorescence studies also showed increased expression of NKA (*SI Appendix*, Fig. S4), although it was not statistically significant (ratio = 1.40, $P = 0.28$). Diabetic principal cells showed decreased *WNK1*. Alternative promoter usage of *WNK1* creates a kidney-specific WNK1 form, which lacks a kinase domain and is found mainly in the DCT, and the long-form, L-WNK1 that negatively regulates surface expression of the K^+ secretory channel, *KCNJ1* (ROMK) in the principal cell (26, 27). The decrease in *NEDD4L*, which negatively regulates ENaC (28), would increase K^+ secretion further. There was also increased expression of aquaporin-3, which is important for concentrating urine and is increased in streptozotocin-induced diabetes (29). The increased expression of AQP3 was also seen in immunofluorescence studies (*SI Appendix*, Fig. S5), but these results were not statistically significant (ratio = 1.70, $P = 0.20$). There was decreased expression of the Na^+/Ca++ exchanger, encoded by *SLC8A1*, which has been reported in experimental models of diabetes (30), and evidence for alteration of SLIT-ROBO signaling with an increase in *ROBO2* and a decrease in *SLIT2*. Interestingly, we detected a statistically significant overlap between a curated list of 908 aldosterone (31–34) and salt-sensitive (35) transcripts with the differentially expressed genes detected in the thick ascending limb, late distal convoluted tubule, and principal cells, suggestive of conserved response to aldosterone signaling (Dataset S10).

A total of 1,874 type A intercalated cells and 693 type B intercalated cells were present in our sample. Type A intercalated cells were enriched for regulation of glucose import in response to insulin stimulus and had decreased expression of *IRS1*, which is associated with genetic susceptibility to type 2 diabetes in Pima Indians (36). Type B intercalated cells were enriched for immune cell activation, including regulation of TNF superfamily cytokine production.

Discussion

In this study, we report a single-nucleus RNA-sequencing dataset of human diabetic nephropathy. Diabetic patients had mild to moderate glomerulosclerosis and interstitial fibrosis, but preserved eGFR, characteristic of early disease. We demonstrated

up-regulation of proangiogenic genes and pathways important for cell motility and cytoskeletal rearrangement by comparing cell-type–specific gene expression. Furthermore, diabetes induced adaptive changes in the thick ascending limb, late distal convoluted tubule, and principal cells that coordinate to promote potassium secretion.

Early changes in gene expression in the thick ascending limb (TAL), late distal convoluted tubule (DCT2), and principal cells collectively promote potassium secretion (Fig. 4) while decreasing paracellular calcium and magnesium reabsorption (Fig. 5). The TAL showed decreased expression of the Na^+/K^+-ATPase (NKA) subunits, *ATP1A1*, *ATP1B1*, and *FXYD2*, and the basolateral potassium channel, *KCNJ16*, in addition to decreased *WNK1*, and its downstream effector, *STK39* (SPAK), which regulate activity of the apical Na^+-K+-2Cl− cotransporter (NKCC2). Decreased NKA, KCNJ16, and NKCC2 activity in the TAL are expected to impair transcellular sodium and potassium reabsorption and decrease paracellular reabsorption of calcium and magnesium. This would be exacerbated by the observed increased expression of the calcium-sensing receptor (*CASR*) and decreased expression of *CLDN16*, which regulates tight junction permeability. These changes were accompanied by increased expression of *SGK1* and decreased expression of an important regulator of ENaC and potassium secretion, *NEDD4L*, in the collecting duct. Interestingly, patients with type 1 or type 2 diabetes and microalbuminuria show significantly decreased activity of NKA in erythrocytes (37, 38) due to glucose-dependent inactivation (39), which is similar to findings in ob/ob mice (40). Reduced NKA activity may result from loss of early compensatory mechanisms and explain the well-known propensity of patients with diabetic nephropathy to develop hyperkalemia and type 4 renal tubular acidosis. In fact, there was a trend toward increased serum potassium levels in diabetic patients, which

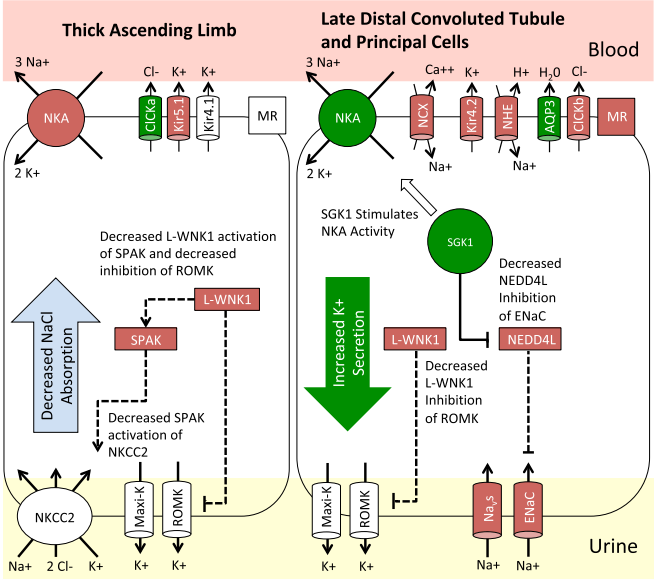

Fig. 4. Coordination of the distal nephron to promote potassium secretion. Genes are depicted as up-regulated (green fill), down-regulated (red fill), or no significant change (white fill) relative to control. The loop of Henle showed decreased expression of the Na^+/K^+-ATPase (NKA) subunits, *ATP1A1*, *ATP1B1*, and *FXYD2*, and the basolateral potassium channel, *KCNJ16* (Kir5.1), in addition to decreased expression of *WNK1* and its downstream effector, *STK39* (SPAK), which regulate activity of the apical Na^+-K+-2Cl− cotransporter (NKCC2). Decreased NKA, KCNJ16, and NKCC2 activity in the loop of Henle are expected to impair transcellular sodium and potassium reabsorption. These changes were accompanied by increased expression of NKA and *SGK1* with decreased expression of an important regulator of ENaC and potassium secretion, *NEDD4L*, in the collecting duct.

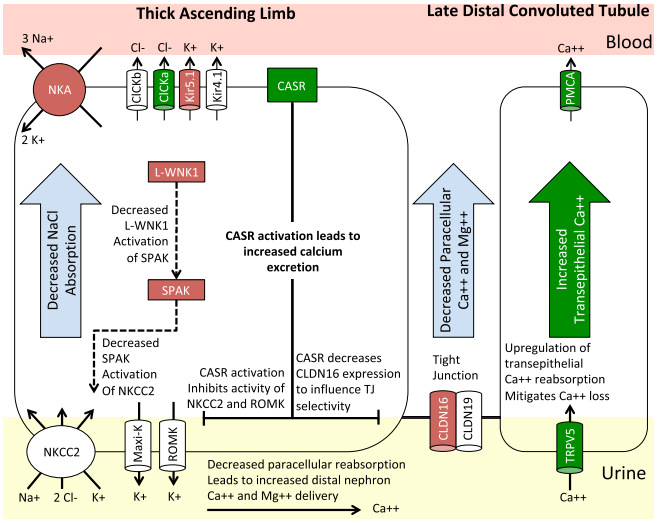

Fig. 5. Decreased paracellular reabsorption of calcium and magnesium. Genes are depicted as up-regulated (green fill), down-regulated (red fill), or no significant change (white fill) relative to controls. Decreased NKA, KCNJ16 (Kir5.1), and NKCC2 activity in the loop of Henle are expected to impair transcellular sodium and potassium reabsorption and decrease paracellular reabsorption of calcium and magnesium. This would be exacerbated by the observed increased expression of the calcium-sensing receptor (*CASR*) and decreased expression of *CLDN16*, which regulates tight junction permeability. Increased expression of the apical calcium-selective channel, *TRPV5*, and the basolateral plasma membrane calcium ATPase (PMCA) in the late distal convoluted tubule likely result as a compensatory mechanism to prevent excessive urinary calcium loss.

may explain the transcriptional changes that promote potassium secretion. Alternatively, this potassium handling response reflects nephron loss with consequent requirement for higher potassium secretion per remaining nephron. In contrast, the late distal convoluted tubule and principal cells showed increased expression of NKA, which promotes potassium secretion via ROMK, and is expected to be up-regulated in response to decreased WNK1 signaling (41). The net effect in the thick ascending limb, late distal convoluted tubule, and principal cells is expected to promote potassium secretion and may represent an adaptive response to early diabetic kidney injury. Alternatively, these changes are a systemic response to elevated serum potassium and aldosterone signaling.

Immune cell infiltration is a well-known feature of diabetic nephropathy (42). We observed an increased number of T cells, B cells, plasma cells, and monocytes in 2 of 3 diabetic samples; however, our study identified relatively few leukocytes, which may reflect the single-nucleus dissociation method used. Infiltrating monocytes expressed markers downstream of IFN gamma signaling (*IFNGR1* and *IFNGR2*), HLA class II histocompatibility antigens (*HLA-DRB1*, *HLA-DRB5*, *HLA-DQA1*), and *TNFRSF1B*, which has been implicated as a biomarker for diabetic nephropathy (43). Comparison of our dataset to publicly available peripheral blood mononuclear datasets showed that infiltrating CD14+ monocytes have increased *TNFRSF21*, which is a urinary marker of diabetic nephropathy progression (15).

A limitation of this study is the relatively small number of patients, and future studies would benefit from increasing the sample size to better delineate interindividual variation and capture the full range of disease severity. Our results lay the foundation for such efforts.

Materials and Methods

Tissue Procurement. Kidney tissue was obtained from patients undergoing partial or radical nephrectomy for renal mass at Brigham and Women's Hospital (Boston, MA) under an established Institutional Review Board

protocol. Nontumor cortical tissue was frozen or retained in OCT for future studies.

Single-Nuclei Isolation and Library Preparation. Nuclei were isolated with lysis buffer, supplemented with protease, and RNase inhibitors. Samples were homogenized, filtered, centrifuged, and resuspended for counting. The 10× Chromium libraries were prepared according to manufacturer protocol (*SI Appendix, Supplemental Text*).

Bioinformatics and Data Analysis. Single-nucleus sequencing data were processed with zUMIs (v2.0). Low-quality barcodes and UMIs were filtered using the internal read filtering algorithm and mapped to the human genome (hg38) using STAR (2.6.0). We quantified unique intronic and exonic reads to generate a raw count matrix, which was imported to Seurat. Genes expressed in >3 nuclei and nuclei with at least 500 genes were retained. Seurat objects were subsequently normalized and scaled. The number of principal components was estimated using the PCElbowPlot function.

An integrated dataset was created using canonical correlation analysis and the RunMultiCCA function with highly variable genes curated from individual Seurat objects. We obtained a new dimensional reduction matrix by aligning the CCA subspaces and performed clustering. Differential gene analysis was performed on individual clusters and visualized with Seurat. Publicly available peripheral blood mononuclear cell datasets (3 k PBMCs from a Health Donor, Cell Ranger 1.1.0 and 4 k PBMCs from a Health Donor, Cell Ranger 2.1.0) were downloaded from the 10× Genomics website and integrated with the leukocyte subset to analyze KRIS markers (44).

Ligand–Receptor Interaction Analysis. To study ligand–receptor interactions, we used a draft network published by Ramilowski et al. (44). We examined glomerular or tubulointerstitial cell types and required that 1) the ligand, receptor, or both were differentially expressed and 2) its cognate pair was expressed in the partner cell type.

Functional Gene Set Enrichment Analysis and Gene Overlap. Gene set enrichment analysis was performed with the R package fgsea with default parameters. Genes were ranked within clusters by multiplying avg_logFC by $-\log_{10}$(p_val) obtained from comparing diabetic and control samples with the FindMarkers function in Seurat. The GO databases were downloaded using msigdbr. A curated list of aldosterone-sensitive genes was compared to cell-type–specific differentially expressed genes using the R package GeneOverlap and default parameters.

Immunofluorescence Studies. Formalin-fixed paraffin-embedded tissue sections were deparaffinized and underwent antigen retrieval. Sections were washed, permeabilized, and incubated overnight with primary antibodies followed by staining with secondary antibodies. Images were obtained by confocal microscopy. AQP3 and ATP1A1 were quantified in ImageJ using the color threshold and measure functions to calculate integrated fluorescence density. Total corrected target immunofluorescence was calculated by subtracting the total principal cell area multiplied by the background fluorescence from the integrated fluorescence density (*SI Appendix, Supplemental Text*).

ACKNOWLEDGMENTS. This work was supported by National Institute of Diabetic and Digestive and Kidney Diseases Diabetic Complications Consortium (https://www.diacomp.org) Grants DK076169 (to B.D.H.), DK115255 (to B.D.H.), 173970 from the Chan Zuckerberg Initiative (to B.D.H.), DK104308 (to S.S.W. and B.D.H.), DK054231 (to P.A.W.), and the Fondation Leducq (to P.A.W.).

1. P. C. Wilson, B. D. Humphreys, Single-cell genomics and gene editing: Implications for nephrology. *Nat. Rev. Nephrol.* **15**, 63–64 (2019).
2. H. Wu, Y. Kirita, E. L. Donnelly, B. D. Humphreys, Advantages of single-nucleus over single-cell RNA sequencing of adult kidney: Rare cell types and novel cell states revealed in fibrosis. *J. Am. Soc. Nephrol.* **30**, 23–32 (2019).
3. H. M. Colhoun, M. L. Marcovecchio, Biomarkers of diabetic kidney disease. *Diabetologia* **61**, 996–1011 (2018).
4. J. S. Lin, K. Susztak, Podocytes: The weakest link in diabetic kidney disease? *Curr. Diab. Rep.* **16**, 45 (2016).
5. H. J. Baelde *et al.*, Gene expression profiling in glomeruli from human kidneys with diabetic nephropathy. *Am. J. Kidney Dis.* **43**, 636–650 (2004).
6. K. I. Woroniecka *et al.*, Transcriptome analysis of human diabetic kidney disease. *Diabetes* **60**, 2354–2369 (2011).
7. J. B. Hodgin *et al.*, Identification of cross-species shared transcriptional networks of diabetic nephropathy in human and mouse glomeruli. *Diabetes* **62**, 299–308 (2013).
8. P. C. Wilson *et al.*, The single-cell transcriptomic landscape of early human diabetic nephropathy. Gene Expression Omnibus. https://www.ncbi.nlm.nih.gov/geo/query/acc.cgi?acc=GSE131882. Deposited 29 May 2019.
9. M. E. Pagtalunan *et al.*, Podocyte loss and progressive glomerular injury in type II diabetes. *J. Clin. Invest.* **99**, 342–348 (1997).
10. H. Y. Dai *et al.*, The roles of connective tissue growth factor and integrin-linked kinase in high glucose-induced phenotypic alterations of podocytes. *J. Cell. Biochem.* **113**, 293–301 (2012).
11. Y. Maeshima, H. Makino, Angiogenesis and chronic kidney disease. *Fibrogenesis Tissue Repair* **3**, 13 (2010).
12. J. F. Navarro-González, C. Mora-Fernández, M. Muros de Fuentes, J. García-Pérez, Inflammatory molecules and pathways in the pathogenesis of diabetic nephropathy. *Nat. Rev. Nephrol.* **7**, 327–340 (2011).
13. 10X-Genomics, Data from "3k PBMCs from a Healthy Donor." 10X Genomics. (2016). https://support.10xgenomics.com/single-cell-gene-expression/datasets/1.1.0/pbmc3k. Accessed 14 April 2019.
14. 10X-Genomics, Data from "4k PBMCs from a Healthy Donor." 10X Genomics. (2017). https://support.10xgenomics.com/single-cell-gene-expression/datasets/2.1.0/pbmc4k. Accessed 14 April 2019.
15. M. A. Niewczas *et al.*, A signature of circulating inflammatory proteins and development of end-stage renal disease in diabetes. *Nat. Med.* **25**, 805–813 (2019).
16. B. Herzog, C. Pellet-Many, G. Britton, B. Hartzoulakis, I. C. Zachary, VEGF binding to NRP1 is essential for VEGF stimulation of endothelial cell migration, complex formation between NRP1 and VEGFR2, and signaling via FAK Tyr407 phosphorylation. *Mol. Biol. Cell* **22**, 2766–2776 (2011).
17. M. Hatting, C. D. J. Tavares, K. Sharabi, A. K. Rines, P. Puigserver, Insulin regulation of gluconeogenesis. *Ann. N. Y. Acad. Sci.* **1411**, 21–35 (2018).
18. N. P. Curthoys, G. Gstraunthaler, Mechanism of increased renal gene expression during metabolic acidosis. *Am. J. Physiol. Renal Physiol.* **281**, F381–F390 (2001).
19. D. H. Jones *et al.*, Na,K-ATPase from mice lacking the gamma subunit (FXYD2) exhibits altered Na+ affinity and decreased thermal stability. *J. Biol. Chem.* **280**, 19003–19011 (2005).
20. Z. Liu *et al.*, Downregulation of NCC and NKCC2 cotransporters by kidney-specific WNK1 revealed by gene disruption and transgenic mouse models. *Hum. Mol. Genet.* **20**, 855–866 (2011).
21. G. Gamba, P. A. Friedman, Thick ascending limb: Tthe Na(+):K (+):2Cl (-) co-transporter, NKCC2, and the calcium-sensing receptor, CaSR. *Pflugers Arch.* **458**, 61–76 (2009).
22. J. Hou *et al.*, Claudin-16 and claudin-19 interact and form a cation-selective tight junction complex. *J. Clin. Invest.* **118**, 619–628 (2008).
23. N. Himmerkus *et al.*, Salt and acid-base metabolism in claudin-16 knockdown mice: Impact for the pathophysiology of FHHNC patients. *Am. J. Physiol. Renal Physiol.* **295**, F1641–F1647 (2008).
24. J. Hou *et al.*, Transgenic RNAi depletion of claudin-16 and the renal handling of magnesium. *J. Biol. Chem.* **282**, 17114–17122 (2007).
25. C. T. Lee, H. Y. Ng, Y. T. Lee, L. W. Lai, Y. H. Lien, The role of calbindin-D28k on renal calcium and magnesium handling during treatment with loop and thiazide diuretics. *Am. J. Physiol. Renal Physiol.* **310**, F230–F236 (2016).
26. J. B. Wade *et al.*, WNK1 kinase isoform switch regulates renal potassium excretion. *Proc. Natl. Acad. Sci. U.S.A.* **103**, 8558–8563 (2006).
27. A. Lazrak, Z. Liu, C. L. Huang, Antagonistic regulation of ROMK by long and kidney-specific WNK1 isoforms. *Proc. Natl. Acad. Sci. U.S.A.* **103**, 1615–1620 (2006).
28. O. Staub *et al.*, WW domains of Nedd4 bind to the proline-rich PY motifs in the epithelial Na+ channel deleted in Liddle's syndrome. *EMBO J.* **15**, 2371–2380 (1996).
29. T. H. Kwon *et al.*, Regulation of collecting duct AQP3 expression: Response to mineralocorticoid. *Am. J. Physiol. Renal Physiol.* **283**, F1403–F1421 (2002).
30. Y. Hattori *et al.*, Diminished function and expression of the cardiac Na+-Ca2+ exchanger in diabetic rats: Implication in Ca2+ overload. *J. Physiol.* **527**, 85–94 (2000).
31. S. B. Poulsen, K. Limbutara, R. A. Fenton, T. Pisitkun, B. M. Christensen, RNA sequencing of kidney distal tubule cells reveals multiple mediators of chronic aldosterone action. *Physiol. Genomics* **50**, 343–354 (2018).
32. R. Soundararajan, T. T. Zhang, J. Wang, A. Vandewalle, D. Pearce, A novel role for glucocorticoid-induced leucine zipper protein in epithelial sodium channel-mediated sodium transport. *J. Biol. Chem.* **280**, 39970–39981 (2005).
33. M. Robert-Nicoud *et al.*, Transcriptome of a mouse kidney cortical collecting duct cell line: Eeffects of aldosterone and vasopressin. *Proc. Natl. Acad. Sci. U.S.A.* **98**, 2712–2716 (2001).
34. P. Fakitsas *et al.*, Early aldosterone-induced gene product regulates the epithelial sodium channel by deubiquitylation. *J. Am. Soc. Nephrol.* **18**, 1084–1092 (2007).
35. E. A. Swanson *et al.*, Salt-sensitive transcriptome of isolated kidney distal tubule cells. *Physiol. Genomics* **51**, 125–135 (2019).
36. P. Kovacs *et al.*, The role of insulin receptor substrate-1 gene (IRS1) in type 2 diabetes in Pima Indians. *Diabetes* **52**, 3005–3009 (2003).
37. A. Djemli-Shipkolye *et al.*, The effects ex vivo and in vitro of insulin and C-peptide on Na/K adenosine triphosphatase activity in red blood cell membranes of type 1 diabetic patients. *Metabolism* **49**, 868–872 (2000).
38. M. Mimura, H. Makino, A. Kanatsuka, T. Asai, S. Yoshida, Reduction of erythrocyte (Na(+)-K+)ATPase activity in type 2 (non-insulin-dependent) diabetic patients with microalbuminuria. *Horm. Metab. Res.* **26**, 33–38 (1994).

39. J. F. Rivelli *et al*., High glucose levels induce inhibition of Na,K-ATPase via stimulation of aldose reductase, formation of microtubules and formation of an acetylated tubulin/Na,K-ATPase complex. *Int. J. Biochem. Cell Biol.* **44**, 1203–1213 (2012).
40. S. Iannello, P. Milazzo, F. Belfiore, Animal and human tissue Na,K-ATPase in obesity and diabetes: A new proposed enzyme regulation. *Am. J. Med. Sci.* **333**, 1–9 (2007).
41. P. A. Welling, Roles and regulation of renal K channels. *Annu. Rev. Physiol.* **78**, 415–435 (2016).
42. R. Pichler, M. Afkarian, B. P. Dieter, K. R. Tuttle, Immunity and inflammation in diabetic kidney disease: Translating mechanisms to biomarkers and treatment targets. *Am. J. Physiol. Renal Physiol.* **312**, F716–F731 (2017).
43. M. E. Pavkov *et al*., Elevation of circulating TNF receptors 1 and 2 increases the risk of end-stage renal disease in American Indians with type 2 diabetes. *Kidney Int.* **87**, 812–819 (2015).
44. J. A. Ramilowski *et al*., A draft network of ligand-receptor-mediated multicellular signalling in human. *Nat. Commun.* **6**, 7866 (2015). Erratum in: *Nat. Commun.* **7**, 10706 (2016).